Geophysical Prospecting, 2003, **51**, 159–166

Inversion for elliptically anisotropic velocity using VSP reflection traveltimes

Z. Zhang,[1]* G. Lin,[2] J. Chen,[1] J.M. Harris[3] and L. Han[4]

[1]*Institute of Geology and Geophysics, Chinese Academy of Sciences, A-11 Da-tun Road, Chao-Yang District, Beijing 100101, China,* [2]*Guangzhou Institute of Geochemistry, Chinese Academy of Sciences, Guangzhou, China,* [3]*Department of Geophysics, Stanford University, Stanford, CA 94305-2215, USA, and* [4]*Department of Geophysics, Jilin University, Changchun, China*

Received June 2002, revision accepted December 2002

ABSTRACT

This paper presents a traveltime inversion approach, using the reflection traveltimes from offset VSP data, to reconstruct the horizontal and vertical velocities for stratified anisotropic media. The inverse problem is reduced to a set of linear equations, and solved by the singular value decomposition (SVD) technique. The validity of this inversion scheme is verified using two sets of synthetic data simulated using a finite-difference method, one for an isotropic model and the other for an elliptically anisotropic model. The inversion result demonstrates that our anisotropic velocity inversion scheme may be applied to both isotropic and anisotropic media. The method is finally applied to a real offset VSP data set, acquired in an oilfield in northwestern China.

INTRODUCTION

The determination of seismic velocity from VSP traveltimes has been the subject of several papers (Stephen and Harding 1983; Stewart 1984; Hardage 1985; Pujol, Burridge and Smithson 1985; Ross and Shah 1987; Schuster 1988; Schuster, Johnson and Trentman 1988; Swift *et al.* 1998; Lizarralde and Swift 1999). These papers have two features in common: (i) using VSP first-arrival times to determine interval velocities; (ii) assuming an isotropic velocity model and ignoring the effects of seismic anisotropy. However, seismic anisotropy is widespread in the earth's crust, induced by thin-layering (Helbig 1983; Thomsen 1986), oriented cracks, fractures, etc. (Hudson 1980). The neglect of seismic anisotropy in inversion may lead to distorted images of the subsurface structure, even misinterpretation. The aim of this paper is to use VSP reflection traveltimes to invert for the anisotropic velocity structure.

Currently, the determination of seismic anisotropy from seismic measurement can be approached in two ways: (i) obtaining either the shear-wave splitting time delay or the polarization of the fast split shear wave, in order to constrain the description of crack or fracture reservoirs (Majer *et al.* 1988; Queen and Rizer 1990; Winterstein and Meadows 1991); (ii) obtaining elastic parameters or anisotropic velocities in anisotropic media (Chapman and Pratt 1992; Pratt and Chapman 1992; Tsvankin and Thomsen 1995). In the latter, the anisotropic tomography technique for cross-hole data was developed to image the structures of five elastic parameters in transversely isotropic media with symmetry about the vertical axis (Winterstein and Paulsson 1990; Michelena, Muir and Harris 1993; de Gopa, Winterstein and Meadows 1994). A generic algorithm was used to invert anisotropic velocities from the first-arrival traveltimes of VSP measurements (Winterstein and Paulsson 1990; de Gopa *et al.* 1994).

Even though elliptical anisotropy is an example of the simplest anisotropy, it still has significance and meaning in seismic exploration (Helbig 1983; Dellinger and Muir 1988). This paper presents an inversion approach to reconstructing the horizontal and vertical velocities in elliptically anisotropic media by using the reflection traveltimes from offset VSP measurements. Our study focuses on the traveltime inversion of an upgoing reflection wave. However, the method can be adapted to the inversion of downgoing wave

*E-mail: zjzhang@mail.c-geos.ac.cn

traveltimes by applying the forward modelling formula and the Jacobian matrix in the inverse problem to the downgoing wave traveltimes.

INVERSION METHOD

Forward calculation of VSP reflection traveltimes

Consider a layered earth model consisting of N layers (Fig. 1) and M VSP receiver points receiving reflections from the Kth reflector. For the ith receiver at depth Z_i and the reflection from the Kth interface, the reflection traveltime can be written as

$$T_i^K = \sum_{j_1=1}^{K-1} \frac{h_{j_1}}{V_{j_1}\cos\alpha_{j_1}} + \frac{\sum_{j=1}^{K_1} h_j - Z_i}{V_{K_1}\cos\alpha_{K_1}} + \frac{h_K}{V_K\cos\alpha_K} + \left(\sum_{j_2=K_1+1}^{K-1} \frac{h_{j_2}}{V_{j_2}\cos\alpha_{j_2}} + \frac{h_K}{V_K\cos\alpha_K}\right)[1-\delta(K_1-K)], \quad (1)$$

and the offset equation is expressed as

$$x_s = \sum_{j_1=1}^{K-1} h_{j_1}\tan\alpha_{j_1} + \left(\sum_{j=1}^{K_1} h_j - Z_i\right)\tan\alpha_{K_1} + h_K\tan\alpha_K + \left(\sum_{j_2=K_1+1}^{K-1} h_{j_2}\tan\alpha_{j_2} + h_K\tan\alpha_K\right)[1-\delta(K_1-K)], \quad (2)$$

where

$$\delta(K_1-K) = \begin{cases} 1, K_1 = K \\ 0, K_1 \neq K \end{cases},$$

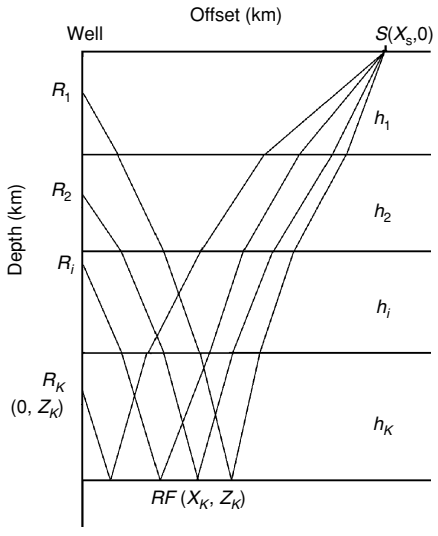

Figure 1 Sketch map of VSP measurement.

h_j is the thickness of the jth layer, and α_j is the ray angle between the ray and the vertical direction in the jth layer. The VSP source is located at the point (x_s, 0), and the ith receiver is located at the K_ith layer. The energy (ray) velocity, V_j, in the jth layer can be written as

$$V_j = \frac{V_{vj}V_{hj}}{\sqrt{V_{vj}^2\sin^2\alpha_j + V_{hj}^2\cos^2\alpha_j}}, \quad (3)$$

where V_{hj} and V_{vj} are the horizontal and vertical velocities, respectively, for the jth layer of an elliptically anisotropic medium. Obviously the parameters such as layer thickness h_j and receiver depth Z_i are known; in order to calculate the reflecting traveltime T_i^K, the ray angle α_j is needed.

Using Snell's law, which states that reflecting and transmitting seismic waves from an interface should satisfy the condition:

$$p = \frac{V_{v1}\sin\alpha_1}{V_{h1}^2} = \frac{V_{v2}\sin\alpha_2}{V_{h2}^2} = \cdots, \quad (4)$$

where p is the ray parameter, and α_i denotes the ray angle for the incident, reflecting or transmitting wave for the ith reflector, the following relationship between the ray angle α_j and offset x_s can be obtained:

$$T_i^K = \sum_{j_1=1}^{K-1} \frac{V_{vj_1}h_{j_1}}{V_{j_1}\sqrt{V_{vj_1}^2 - p^2V_{hj_1}^4}} + \frac{V_{vK_1}\left(\sum_{j=1}^{K_1} h_j - Z_i\right)}{V_{K_1}\sqrt{V_{vK_1}^2 - p^2V_{hK_1}^4}} + \frac{V_{vK}h_K}{V_K\sqrt{V_{vK}^2 - p^2V_{hK}^4}} + \left(\sum_{j_2=K_1+1}^{K-1} \frac{V_{vj_2}h_{j_2}}{V_{j_2}\sqrt{V_{vj_2}^2 - p^2V_{hj_2}^4}} + \frac{V_{vK}h_K}{V_K\sqrt{V_{vK}^2 - p^2V_{hK}^4}}\right)[1-\delta(K_1-K)], \quad (5)$$

and

$$x_s = \sum_{j_1=1}^{K-1} \frac{V_{hj_1}^2 ph_{j_1}}{\sqrt{V_{vj_1}^2 - p^2V_{hj_1}^4}} + \frac{V_{hK_1}^2\, p\left(\sum_{j=1}^{K_1} h_j - Z_i\right)}{\sqrt{V_{vK_1}^2 - p^2V_{hK_1}^4}} + \frac{V_{hK}^2\, ph_K}{\sqrt{V_{vK}^2 - p^2V_{hK}^4}} + \left(\sum_{j_2=K_1+1}^{K-1} \frac{V_{hj_2}^2 ph_{j_2}}{\sqrt{V_{vj_2}^2 - p^2V_{hj_2}^4}} + \frac{V_{hK}^2\, ph_K}{\sqrt{V_{vK}^2 - p^2V_{hK}^4}}\right)[1-\delta(K_1-K)]. \quad (6)$$

The ray parameter p is defined by the ray angle of the first layer in (4). That is, if the ray angle α_1 is known, the reflection traveltime T_i^K can be calculated from (5). The first incident ray angle α_1 is obtained by trial and error.

Inversion procedure

The inversion is performed layer by layer. To invert the Kth layer, it is assumed that the velocity parameters above the Kth layer and the initial velocity model of the objective layer (V_{vk}, V_{bk}, for the vertical and horizontal velocities, respectively) are known. The misfit function of the upgoing reflection traveltime for the ith receiver is written as

$$\Delta T_i^K \equiv T_i^K - T_{i0}^K = \frac{\partial T_i^K}{\partial V_{vK}}\Delta V_{vK} + \frac{\partial T_i^K}{\partial V_{bK}}\Delta V_{bK} + O(V_{vK}, V_{bK}), \tag{7}$$

where T_{i0}^K is the calculated reflection traveltime from the Kth layer for the ith receiver, and $O(V_{vK}, V_{bK})$ represents the terms higher than first-order derivatives.

For the M receivers that record the reflection from the Kth reflecting interface, (7) can be represented in matrix form as

$$\Delta\mathbf{T} = \mathbf{A}\Delta\mathbf{V}, \tag{8}$$

where $\Delta\mathbf{T}$ is the residual vector, $\Delta\mathbf{V} = [\Delta V_{vK}, \Delta V_{bK}]^{\mathrm{T}}$ is the unknown velocity vector, and $\mathbf{A}$ is an $M \times 2$ Jacobian matrix. The elements in the Jacobian matrix are the traveltime derivatives with respect to vertical and horizontal velocities and are given by

$$\frac{\partial T_i^K}{\partial V_{vK}} = -\left[2h_K + \delta(K_1 - K)\left(\sum_{j=1}^{K-1} h_j - Z_i\right)\right] \Big/ C_1 V_{bK}^3. \tag{9}$$

and

$$\frac{\partial T_i^K}{\partial V_{bK}} = -\left[2h_K + \delta(K_1 - K)\left(\sum_{j=1}^{K-1} h_j - Z_i\right)\right] \tan^2\alpha_K \Big/ C_1 V_{bK}^3, \tag{10}$$

where

$$C_1 = \frac{1}{\sqrt{\tan^2\alpha_K / V_{bK}^2 + 1/V_{vK}^2}}.$$

The linear equation (8) can be solved using the singular value decomposition (SVD) method

$$\mathbf{A} = \mathbf{U}\begin{bmatrix} w_1 & 0 \\ 0 & w_2 \end{bmatrix}\mathbf{V}^{\mathrm{T}}. \tag{11}$$

The anisotropic velocity model is updated by

$$\begin{aligned} V_{vK}^{n+1} &= V_{vK}^n + \Delta V_{vK}, \\ V_{bK}^{n+1} &= V_{bK}^n + \Delta V_{bK}, \end{aligned} \tag{12}$$

where n denotes the iteration number, and model updates are given by

$$\begin{bmatrix} \Delta V_{vK} \\ \Delta V_{bK} \end{bmatrix} = \mathbf{V}\mathrm{diag}\left[\frac{1}{w_j}\right]\mathbf{U}^{\mathrm{T}}\Delta\mathbf{T}. \tag{13}$$

Iteration continues until the sum $(|\Delta V_{vK}| + |\Delta V_{bK}|)$ of the absolute updates is less than the error expectancy. The set of values, V_{HK} and V_{VK}, is then taken as the final result for the horizontal and vertical velocities of the elliptically anisotropic medium.

SYNTHETIC AND REAL DATA EXAMPLES

The inversion scheme is illustrated using two sets of synthetic VSP data, followed by application to a real VSP data set recorded in an oilfield in northwestern China. In the following examples, the initial model is taken to be the output of isotropic first-arrival traveltime inversion, namely, the initial model consists of isotropic layers.

The first model (Model I), consisting of 10 isotropic layers (Fig. 2), represents a deep VSP with a maximum depth of 2000 m. The offset is set at 1000 m and the reflectors are located at depth intervals of 200 m, starting at a depth of 200 m and ending at 2000 m. The P-wave velocities of the 10 isotropic media from shallow to deep (from V_1 to V_{10}) are assumed to be 2300, 2500, 2000, 2700, 2400, 2600, 2900, 3300, 3500 and 3000 m/s, respectively. There are two lower-velocity layers (LVL) (the third and fifth layers) in this model.

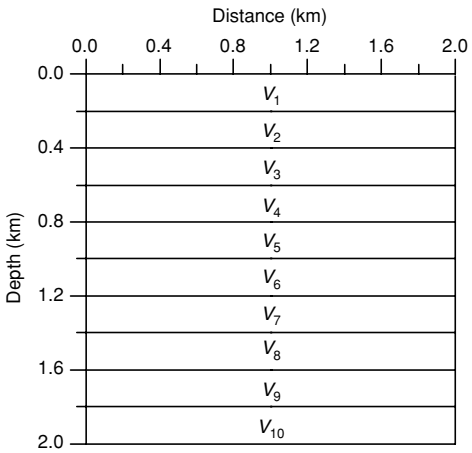

Figure 2 Stratified earth model for synthetic VSP modelling.

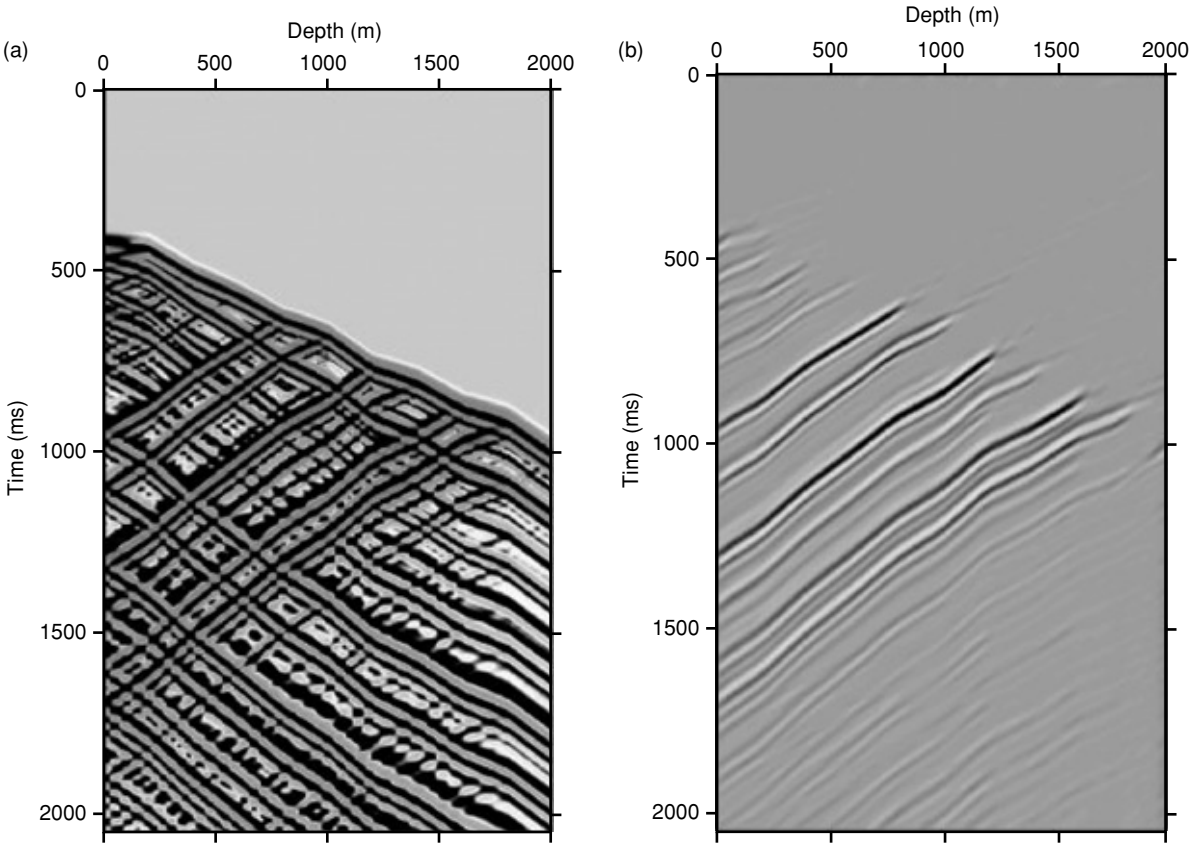

Figure 3 Model I: (a) synthetic VSP; (b) upgoing wavefield after wavefield separation.

For the synthetic VSP modelling, the earth model is divided into 100×200 cells, in which the horizontal and vertical intervals are set at 10 m. The seismic trace interval is 10 m, and receivers are placed at depths from 10 m to 2000 m in the VSP model. The offset of VSP measurement is 1000 m and the source is assumed to be a Ricker wavelet with a dominant frequency of 50 Hz. Figure 3(a) shows the synthetic VSP seismogram calculated using the finite-difference method (Zhang, Wang and Harris 1999). Figure 3(b) is the upgoing wavefield, after *F–K* wavefield separation.

First, the inversion of isotropic velocities is performed to obtain the image of the velocity structure (Fig. 4), using the reflection traveltimes from the offset VSP. Then, using the inversion result of isotropic inversion as the initial model for the anisotropic velocity inversion, the horizontal and the vertical velocities are obtained (Fig. 5a). The anisotropic factor (the ratio of horizontal velocity to vertical velocity) is shown in Fig. 5(b).

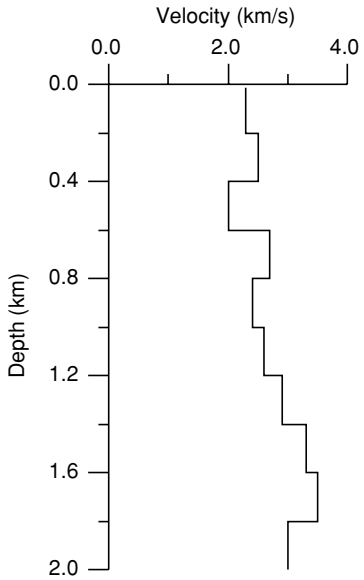

Figure 4 Velocity function obtained from inversion of upgoing reflection traveltimes, based on an isotropic model assumption.

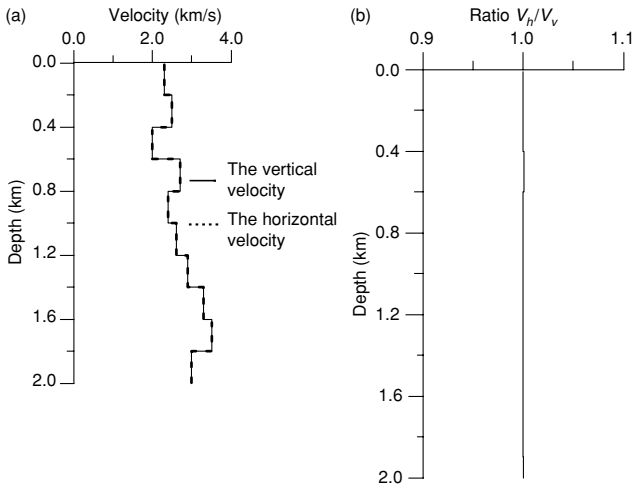

Figure 5 (a) Horizontal and vertical velocities obtained from traveltime inversion based on the anisotropic model assumption. (b) Anisotropy factor (V_h/V_v) versus depth.

Although the velocity image from the isotropic velocity inversion matches the real velocity structure well, a good match between the velocity image obtained from the elliptically anisotropic inversion and the real velocity structure is also required. Characteristically, the horizontal and vertical velocities are nearly equal to the real velocities, and the ratio is close to unity. This demonstrates that, for an anisotropic velocity inversion, an anisotropic medium cannot be considered as a series of isotropic layers.

The second example (Model II) is a stratified, elliptically anisotropic medium, with the same geometrical parameters as in Model I, except that the stratified layers are elliptically anisotropic. The vertical and horizontal velocities for each layer are assumed to be 2000 and 2300 m/s for the first layer, 2300 and 2500 m/s for the second layer, 2400 and 2500 m/s for the third layer, 2700 and 2900 m/s for the fourth layer, 2400 and 2500 m/s for the fifth layer, 2500 and 2600 m/s for the sixth layer, 2400 and 2300 m/s for the seventh layer, 2700

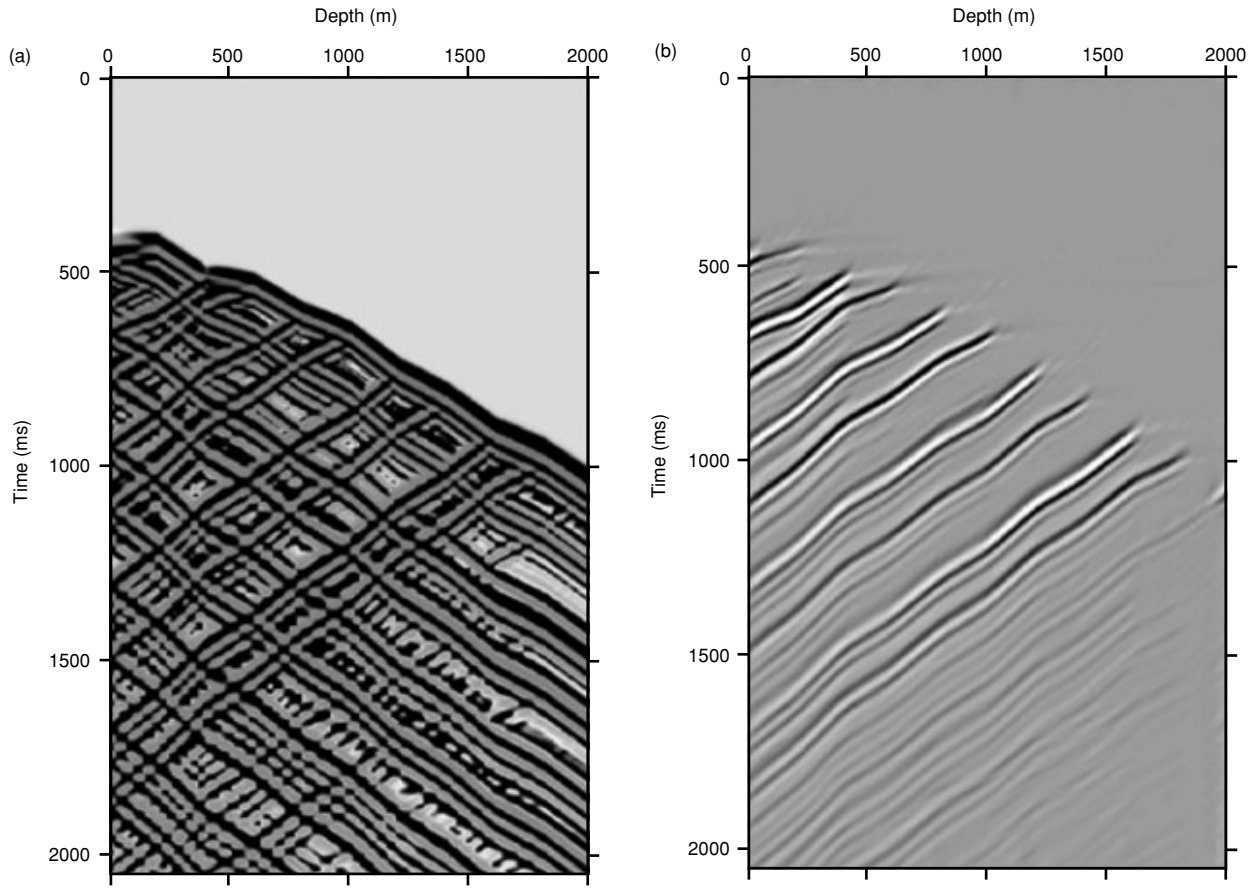

Figure 6 Model II: (a) synthetic VSP; (b) upgoing wavefield after wavefield separation.

and 2900 m/s for the eighth layer, 2800 and 3000 m/s for the ninth layer, and 3000 and 3300 m/s for the bottom layer. The synthetic VSP and its upgoing wavefield are shown in Figs 6(a) and 6(b).

Similarly to the processing of Model I, we perform an isotropic velocity inversion (Fig. 7) and then an anisotropic velocity inversion (Fig. 8). Obviously, the velocity image of Fig. 7 does not match the real velocity model; that is, the isotropic velocity inversion method does not fit the elliptically anisotropic medium. However, the elliptically anisotropic velocity inversion not only gives a good result in this case, but can also be applied satisfactorily to isotropic media, as in Model I.

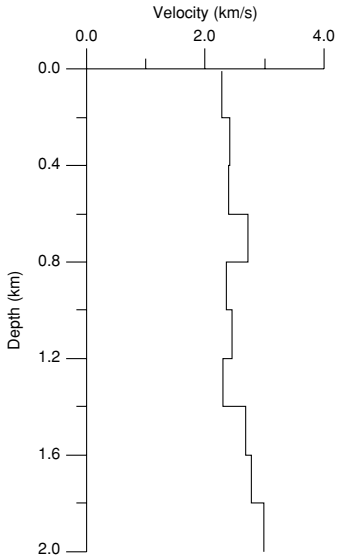

Figure 7 Velocity function obtained from inversion of upgoing reflection traveltimes, based on an isotropic model assumption.

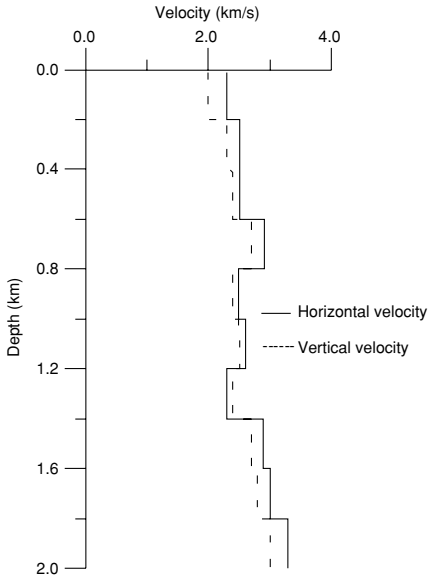

Figure 8 Horizontal and vertical velocities obtained from traveltime inversion, assuming elliptical anisotropy.

Figure 9(a) shows a real VSP measurement taken from an oilfield in northwestern China. In this VSP with an offset of 1000 m, 219 receivers are deployed for the measurements in the well. The trace interval is 5 m. The upgoing wavefield, after wavefield separation using *F–K* filtering for the real data, is shown in Fig. 9(b).

The velocity structure, using the isotropic velocity inversion method, is shown in Fig. 9(c). The horizontal and vertical velocity structures, obtained by using the anisotropic velocity method presented here, are shown in Fig. 9(d). The ratio of horizontal velocity to vertical velocity is shown in Fig. 9(e), from which we can see that seven layers out of a total of 10 possess elliptical anisotropy. The most anisotropic layer is the second layer, with anisotropy of up to 40%.

CONCLUSION

We present a traveltime inversion approach that reconstructs horizontal and vertical velocities in elliptically anisotropic media using reflection traveltimes in offset VSPs. The inverse problem, which minimizes the misfit between the VSP measurement and calculated traveltimes, is reduced to a set of linear equations, which can be solved by the SVD technique. The method is applicable to both isotropic media and anisotropic media. If the anisotropic velocity inversion is performed on data from an actual isotropic structure, the resulting inversion image will not be distorted by the inversion algorithm. The method developed here may be extended to more complex inhomogeneous anisotropy with different symmetry axes and to 3D cases.

ACKNOWLEDGEMENTS

This research was financially supported by the Outstanding Youth Scientist Project of the Chinese National Nature Science Foundation (grant no. 49852108) and the Chinese Academy of Sciences (KXCX2-109). The real VSP data set was provided by the Institute of Geophysical Prospecting for Petroleum, Chinese Newstar Petroleum Company. Constructive suggestions from the reviewers were appreciated.

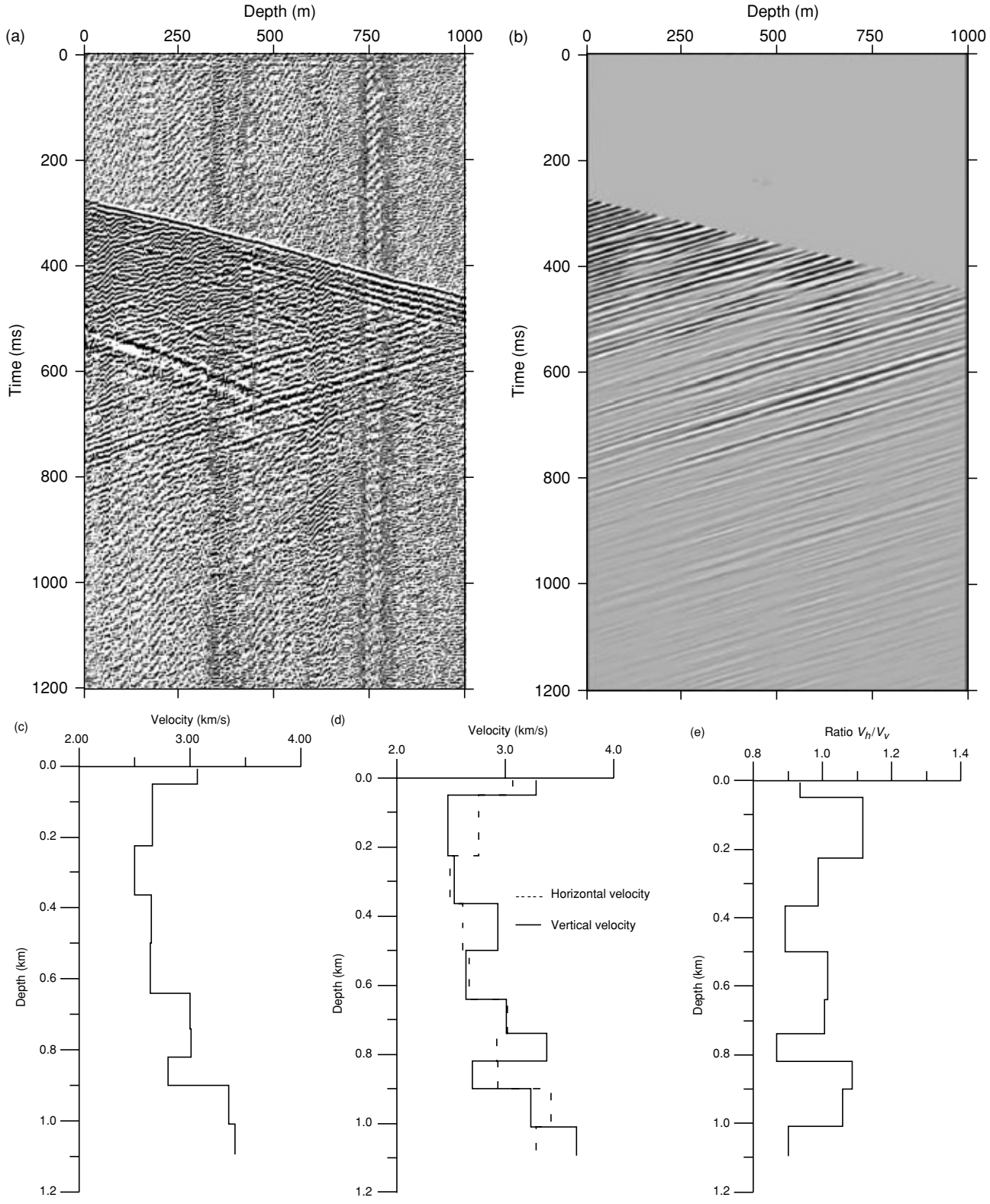

Figure 9 (a) Real VSP data. (b) Upgoing wavefield. (c) Isotropic velocity inversion. (d) Anisotropic velocity inversion. (e) Anisotropy factor versus depth.

REFERENCES

Chapman C.H. and Pratt R.G. 1992. Traveltime tomography in anisotropic media: theory. *Geophysical Journal International* **109**, 1–19.

Dellinger J. and Muir F. 1988. Imaging reflections in elliptically anisotropic media. *Geophysics* **53**, 1616–1618.

de Gopa S., Winterstein D.F. and Meadows M.A. 1994. Comparison of *P*- and *S*-wave velocities and *Q*'s from VSP and sonic log data. *Geophysics* **59**, 1512–1529.

Hardage B.A. 1985. *Vertical Seismic Profiling, Part A: Principles*, 2nd edn. Pergamon Press Inc.

Helbig K. 1983. Elliptical anisotropy – its significance and meaning. *Geophysics* **48**, 825–832.

Hudson J.A. 1980. Overall properties of a cracked solid. *Mathematical Proceedings of the Cambridge Philosophical Society* **88**, 371–384.

Lizarralde D. and Swift S. 1999. Smooth inversion of VSP traveltime data. *Geophysics* **64**, 659–661.

Majer E.L., McEvilly T.V., Eastwood F.S. and Myer L.R. 1988. Fracture detection using *P*-wave and *S*-wave vertical seismic profiling at The Geysers. *Geophysics* **53**, 76–84.

Michelena R.J., Muir F. and Harris J.M. 1993. Anisotropic traveltime tomography. *Geophysical Prospecting* **41**, 381–412.

Pratt R.G. and Chapman C.H. 1992. Traveltime tomography in anisotropic media: application. *Geophysical Journal International* **109**, 20–37.

Pujol J., Burridge R. and Smithson S.B. 1985. Velocity determination from offset vertical seismic profiling data. *Journal of Geophysical Research* **90**, 1871–1880.

Queen J.H. and Rizer W.D. 1990. An integrated study of seismic anisotropy and the natural fracture system at the Conoco borehole test facility, Kay County, Oklahoma. *Journal of Geophysical Research* **95**, 11255–11274.

Ross W.S. and Shah P.M. 1987. Vertical seismic profile reflectivity: ups and downs. *Geophysics* **52**, 1149–1154.

Schuster G.T. 1988. An analytic generalized inverse for common-depth-point and vertical seismic profile traveltime equations. *Geophysics* **53**, 314–325.

Schuster G.T., Johnson D.P. and Trentman D.J. 1988. Numerical verification and extension of an analytic generalized inverse for common-depth-point and vertical-seismic-profile traveltime equations. *Geophysics* **53**, 326–333.

Stephen R.A. and Harding A.J. 1983. Travel time analysis of borehole seismic data. *Journal of Geophysical Research* **88**, 8289–8298.

Stewart R.R. 1984. VSP interval velocities from traveltime inversion. *Geophysical Prospecting* **32**, 608–628.

Swift S.A., Lizarralde D., Stephen R.A. and Hoskins H. 1998. Velocity structure in upper ocean crust at Hole 504B from vertical seismic profiles. *Journal of Geophysical Research* **107**, 15361–15376.

Thomsen L. 1986. Weak elastic anisotropy. *Geophysics* **51**, 1954–1966.

Tsvankin I. and Thomsen L. 1995. Inversion of reflection traveltimes for transverse isotropy. *Geophysics* **60**, 1095–1107.

Winterstein D.F. and Meadows M.A. 1991. Changes in shear-wave polarization azimuth with depth in Cymric and Railroad Gap oilfield. *Geophysics* **56**, 1349–1364.

Winterstein D.F. and Paulsson B.N.P. 1990. Velocity anisotropy in shale determined from crosshole seismic and VSP data. *Geophysics* **55**, 470–479.

Zhang Z.-J., Wang G.-J. and Harris J.M. 1999. Multi-component wavefield simulation in viscous extensively dilatancy anisotropic media. *Physics of the Earth and Planetary Interiors* **114**, 25–38.